ISSN: 2472-3703 DOI: 10.6911/WSRJ.202105_7(5).0022

Analysis and Comparison of Quasi-Elastic Neutron Scattering (QENS) Spectra Model

Cunxin Xiao[1], Jie Zhang[1], Yuhang Chen[1] and Hua Li[1, a, *]

[1]Department of Physics, Jinan University, Guangzhou, China

[a]Corresponding author E-mail: tlihua@jnu.edu.cn

Abstract

The Quasi-Elastic Neutron Scattering (QENS) experiment is a novel method to study confined water dynamics by measuring the neutron energy transfer (E)and scattering vector (Q) after the neutron interacts with the sample target. By adopting a suitable theoretical model and performing nonlinear least-squares fitting analysis on the Quasi-Elastic Neutron scattering spectra, the relevant physical parameters describing the water dynamics can be obtained, and then the constrained water dynamics in the sample can be detected. There are many types of Quasi-Elastic Neutron Scattering spectra fitting analysis models, and the fitting effects of different models and the relevant physical parameters obtained to characterize water dynamic information are not the same. This paper uses the Jump-diffusion and Rotating-diffusion Model (JRM) and the revised Jump-diffusion and Rotating-diffusion Model (rJRM) to fit the QENS spectra of pure magnesium silicate (M-S-H) and pure calcium silicate (C-S-H) samples, respectively. The measurement temperatures of QENS spectra from M-S-H and C-S-H samples are 210K up to 280K and 230K up to 280K, respectively, the E ranges from -120 to $120\,\mu ev$ and the Q value 0.3 $Å^{-1}$~1.9 $Å^{-1}$. Different physical parameters describing the dynamic information of confined water can be obtained by using the two models for QENS spectra fitting analysis. Compared with the JRM model, the physical parameters obtained by using the rJRM model are more comprehensive, and it is suitable for all neutron energy transfer and scattering vector measurements. From the qualitative point of view, the QENS spectra fitting curve of rJRM model is more consistent with the original data points. From the quantitative point of view, the chi-square value fitted by the rJRM model is more consistent with the mathematical statistics law than the JRM model, and the time required for nonlinear fitting is shorter.

Keywords

Cement samples; Data analysis of QENS spectra; Dynamics of water; Jump-diffusion and Rotation-diffusion Model (JRM); Quasi-Elastic Neutron Scattering (QENS); Revised Jump-diffusion and Rotation-diffusion Model (rJRM).

1. INTRODUCTION

Cement is a widely used building material around the world. When water and cement ash are mixed and left for some time, the mixture will turn into hard concrete blocks. This cement block, called concrete, is a complex system of inorganic colloids. Ordinary Portland Cement (OPC) is the most commonly used. The main products of portland cement hydration process are Calcium-silicate-hydrate (C-S-H) and Calcium-hydroxide(CH) [1, 2]. C-S-H plays a key role in the strength and durability of cement slurry, which is the main cement binder, accounting for 50% to 70% of the total mass of cement. Although conventional Portland cement is widely used, the

ISSN: 2472-3703 DOI: 10.6911/WSRJ.202105_7(5).0022

process of making and using Portland cement produces a large amount of carbon dioxide, which is not conducive to sustainable development globally [3]. Therefore, attention is being paid to new environmentally friendly cement, among which magnesium-based cement has attracted attention because of its low carbon dioxide emissions during manufacturing [4]. The main components of Magnesia-based cement are Magnesium-silicate-hydrate (M-S-H) and Magnesium-hydroxide (MH). Since both M-S-H and C-S-H are colloidal materials, there are two types of water in the pores of M-S-H and C-S-H nano gels during the long hydration process of cement [2, 3]: One is bound water, which becomes part of the pore structure itself by chemical combination of water molecules and cannot move freely. The other type is confined water, which is in a restricted or strongly restricted state in the micro-nano pore and can move freely [5]. The ratio of bound water and the dynamics of water in the confined state affect the macroscopic mechanical properties of cement, such as strength and durability. Therefore, it is of great significance to study the microstructure of cement hydration and the water content and water dynamics limited by micro and nano-pores for understanding and improving cement performance [6-9]. Although it is difficult to study the micro-dynamics of water in nanoscale pores, since the incoherent scattering cross-section of neutrons and hydrogen atoms are much larger than those of other atoms($\sigma_{inc}(H) = 80.26bar$) [10], the Quasi-Elastic Neutron Scattering (QENS) experiment of cement samples is very suitable for studying the microscopic dynamics of confined water in the sample. The information obtained by QENS spectra is mainly the incoherent scattering information of neutrons and hydrogen atoms, including the dynamic information of water molecules containing two hydrogen atoms.

There are mainly three theoretical models for the QENS spectra analysis of cement samples in the past: the relaxed cage model (RCM) [11, 12], the empirical diffusion model (EDM) [13], and the Jump-diffusion and rotation-diffusion model (JRM) [7, 14]. The RCM model only considers the translational diffusion of water molecules, while the EDM model considers the translational diffusion and partial rotational diffusion of water molecules ($l = 0, 1$). The JRM model considers the translational and rotational diffusion more comprehensively ($l = 0, 1, 2, 3$). Although all the three models used to fit QENS spectra data, none of which can give very well fitted QENS spectra both for $Q \le 1 \text{Å}^{-1}$ and $Q \ge 1 \text{Å}^{-1}$ in the neutron energy transform larger than $\pm 50 \mu ev$. Later, Le p et al. proposed a new fitting model (new global model) [15], based on the RCM model. The neutron energy transfer range extended to $\pm 100 \mu ev$, but the fitted results were not satisfactory for $Q \ge 1.3 \text{Å}^{-1}$.

Therefore, to fit and analyze the high-resolution QENS spectral data more comprehensively, some of the authors in this paper revised the Jump-diffusion and rotation-diffusion model (JRM) and obtained the rJRM model [16]. The improvement of rJRM model compared with JRM model has two points: the first is to add the contribution of movable water to the elastic part based on considering the contribution of immovable water to the elastic part [17, 18]; the second is to increase the contribution of the coherent neutron scattering cross-section to the rotational diffusion in the Sears expansion based on taking into account the incoherent neutron scattering cross-section.

In this paper, the JRM model and the rJRM model of QENS spectra fitting are firstly compared and introduced. Then, based on the high-resolution QENS spectra data of C-S-H and M-S-H samples, the JRM model and the rJRM model are respectively used to carry out nonlinear least-squares fitting for the QENS spectra of the two samples within the range of all measured data($Q = 0.3 - 1.9 \text{Å}^{-1}$, $E = \pm 120 \mu ev$). Due to different fitting models, fitting effects and related physical quantities that describe water dynamics in cement samples obtained by fitting are also different. Therefore, the dynamic characteristics of water molecules in Nanogel pores under different temperatures are revealed from different angles. Then the JRM and rJRM models are compared qualitatively and quantitatively from the Angle of the fitting results and statistical

ISSN: 2472-3703 DOI: 10.6911/WSRJ.202105_7(5).0022

analysis, which provides the corresponding practical basis for the improvement of the QENS spectral data fitting model.

2. MATERIALS

In this paper, two kinds of cement samples were used, namely pure M-S-H sample and pure C-S-H sample, and the related information of the high-resolution QENS spectra data was listed in Table 1. The QENS spectra experiments of these two cement samples were completed on the backscattering silicon spectrometer (BASIS) [19], a high-resolution backscatter at the Spallation Neutron Source (SNS) in Oak Ridge National Laboratory (ORNL). BASIS is an effective tool to study the diffusion and relaxation process of confined water molecules [20]. The experimental data is provided by the working group of Professor Sow-Hsin Chen, Department of Nuclear Science and Engineering, Massachusetts Institute of Technology [21, 22]. Both samples were aged at room temperature for 28 days before the experiment, All these samples were prepared according to the synthetic approach and an equilibrium water-to-solid ratio of 0.3 (w/s = 0.3). In the experimental measurement, the energy resolution of BASIS is $3.4\mu ev$, the neutron energy transfer measured by BASIS is from $-120\mu ev$ to $120\mu ev$, the corresponding dynamic time is on the order of 10 ps to 1 ns, and the detected neutron scattering vector Q ranges from 0.3 $Å^{-1}$ to 1.9 $Å^{-1}$, the measured temperature was from 210 K to 280 K for the M-S-H paste samples, and from 230 K to 280 K for the C-S-H paste sample. Besides, the sample-specific instrument resolution function was collected for each sample at 4 K temperature.

Table 1. QENS spectra data of two groups of cement samples

Sample	Temperature range (K)	Information
Pure M-S-H	210 – 280	water-to-solid ratio(w/s): 0.3 Sample aging time(day): 28 Neutron energy transfer (μev): ±120 Neutron scattering vector (Å-1): 0.3 - 1.9
Pure C-S-H	230 - 280	Energy resolution function ambient temperature: 4 K

3. FITTING METHODS OF QEMS SPECTRA

3.1. The Jump-diffusion and Rotation Diffusion Model

The jump-diffusion and rotation diffusion model (JRM) has already been used to fit QENS spectra by Bordallo et al. [7] in 2006. In recent years, we have also adopted this model to analyze QENS spectra data, but with a slight modification, the neutron scattering intensity $S(Q,\omega)$ is converted into $S(Q,E)$. JRM can comprehensively describe the diffusion motion of confined water molecules, which includes the rotational diffusion motion of water molecules around their center of mass (rotational diffusion function $S_R(Q,E)$) and the long-range translational diffusion motion (translational diffusion function $S_T(Q,E)$). Since the relaxation times of these two kinds of diffusion motions are of different magnitude, it can be assumed that they are independent of each other [7, 23], Then the convolution of the translation and rotation functions is obtained [24]. Therefore, the JRM model that takes into account rotational diffusion and translational diffusion is expressed as:

$$S(Q,E) = A\{C\delta(E) + (1-C)[S_T(Q,E) \otimes S_R(Q,E)]\} \otimes R(Q,E) \quad (1)$$

ISSN: 2472-3703 DOI: 10.6911/WSRJ.202105_7(5).0022

Where Q is neutron scattering vector (momentum exchange), E the neutron energy transfer, A the Debye-Waller factor (DWF), $\delta(E)$ the Dirac delta function, $\otimes$ the convolution operator, and $R(Q,E)$ the resolution function measured by the QENS experiment. C the ratio of immobile water, denotes the proportion of chemically bound water bound in a hydrogen compound, and is a factor of the elastic part of the QENS spectra, $(1-C)$ is the proportion of free water that can be moved. It exists in nanopore or adsorbed on the surface of hydration products and is a factor of non-elastic components of QENS spectra. Thus, the neutron scattering intensity $S(Q,E)$ is composed of elastic scattering intensity and inelastic scattering intensity [10].

In Eq. (1), the DWF [18], which represents vibration motion, is expressed as:

$$A = \exp(-\frac{1}{3}\langle u^2 \rangle Q^2) \tag{2}$$

Where $\langle u^2 \rangle$ is the mean square displacement (MSD).

The translational diffusion function $S_T(Q,E)$ is usually modeled by a Lorentzian with a half-width at half-maximum (hwhm) $\Gamma_T(Q)$ as:

$$S_T(Q,E) = \frac{1}{\pi}\frac{\Gamma_T(Q)}{\Gamma_T^2(Q)+E^2} \tag{3}$$

Where according to the model of Singwi and Sjölander [25], the $\Gamma_T(Q)$ contains the broadening information of QENS spectra, which can be expressed as:

$$\Gamma_T(Q) = \frac{]D_tQ^2}{1+D_tQ^2\tau_0} \tag{4}$$

Where] is the Plank constant, D_t the self-diffusion coefficient (translational diffusion coefficient), and τ_0 the average translational residence time between two jumps

The local rotational motion of water molecules can be described by a classical model of a rotating sphere of radius a. Therefore, the rotational component $S_R(Q,E)$ can be expressed by the Sears expansion as [7, 24, 26]:

$$S_R(Q,E) = j_0^2(Qa)\delta(E) + \frac{1}{\pi}\sum_{i=1}^{3}(2l+1)j_i^2(Qa)\frac{l(l+1)]D_r}{[l(l+1)]D_r]^2+E^2} \tag{5}$$

Where a is the radius of the rotating sphere model, and it is taken from the O-H distance (0.98 Å) in a water molecule[7], $j_l(l=0,1,2,3)$ the l-order spherical Bessel function, D_r the rotational diffusion coefficient, depends on the rotational relaxation time τ_r by $\tau_r = 1/6D_r$.

3.2. The Revised Jump-diffusion and Rotation Diffusion Model

In Eq.(1) of the JRM model, The elastic fraction of QENS spectra only takes into account the contribution of immovable water, but in practice, movable water also contributes to the elastic

ISSN: 2472-3703 DOI: 10.6911/WSRJ.202105_7(5).0022

part of QENS spectra [18, 27]. Besides, the JRM model does not take into account the coherent scattering of neutrons and hydrogen atoms, and the coherent scattering of neutrons affects the rotation of water molecules. Therefore, the rJRM model is derived by taking into account the contribution of movable water to the elastic part and the influence of neutron coherent scattering on the Sears expansion in the rotation function [16].

In the rJRM model, considering the contribution of movable water to the elastic part of QENS spectra, the translational diffusion function of water molecules can be modified from Eq. (3) as follows:

$$S_T(Q,E) = P(Q)\delta(E) + [1-p(Q)]\frac{1}{\pi}\frac{\Gamma_T(Q)}{\Gamma_T^2(Q)+E^2}, \quad P(Qa_0) = [\frac{3j_1Q(a_0)}{Q(a_0)}]^2 \tag{6}$$

Where $P(Qa_0)$ represents elastic translational intensity from mobile water confined inside a pore with radius a_0 [17,18,28], and j_1 the first-order spherical Bessel function.

In the rJRM model, taking into account the contribution of neutron coherent scattering to the rotational diffusion function, the rotational diffusion function of water molecules is modified from Eq. (5) as:

$$S_R(Q,E) = x\{b_0^2 j_0^2(Qa)\delta(E) + \frac{1}{\pi}\sum_{l=1}^{3}(2l+1)b_l^2 j_l^2(Qa)\frac{l(l+1)]D_r}{[l(l+1)]D_r]^2+E^2}\} \tag{7}$$

The b_l^2 is calculated by $b_l^2 = \begin{cases} 4a_{coh}^2 + 2(1-\eta)a_{inc}^2, & l \text{ is even} \\ 2(1+\eta)a_{inc}^2, & l \text{ is old} \end{cases}$. Where b_l^2 is the neutron scattering length, including the coherent neutron scattering length a_{coh} and the incoherent neutron scattering length a_{inc}, their related values are listed in Table 2. At the same time, the nuclear statistical effect coefficient η of the neutron cross-section is also considered in the neutron scattering length, the η value ranges from 0 to 1, In this paper, η is set as 0.95. x is a parameter to offset the dimension of b_l^2 in the rJRM.

Table 2. The squared values of neutron scattering length

material	H2O	H2	O2
a_{coh}^2 (barn)	0.307	0.142	0.33
a_{inc}^2 (barn)	6.35	6.34	0.02

3.3. Least chi-square Fitting

In this paper, JRM model and rJRM model were used to fit QENS spectral data. The chi-square calculation formula [29] based on the two models is as follows:

$$\chi^2 = \sum_{i=1}^{n}\frac{[S_i(Q,E) - S_i^{'}(Q,E)]^2}{\sigma_i^2} \tag{8}$$

ISSN: 2472-3703 DOI: 10.6911/WSRJ.202105_7(5).0022

Where n is the number of measured values, $S_i(Q,E)$ the experimental data of QENS spectra (measured value), $S_i^{'}(Q,E)$ the QENS spectra fitting value (theoretical value), and σ_i the measured value error. Adjust the model parameters to minimize the chi-square.

If the model can describe the experimental data well (there is no systematic deviation of the model, only the statistical error of the experimental measurement), then χ^2 in Eq.(8) approximately obeys the chi-square distribution with ($n-1$) degrees of freedom, and its mathematical expectation as $E(\chi^2)=n-1$, and the variance as $D(\chi^2)=2(n-1)$, which means that the chi-square value χ^2 is distributed between $(n-1)\pm 2\sqrt{2(n-1)}$ with a 95% probability[30]. If the model cannot describe the experimental data well, the χ^2 in Eq.(8) is too large, which will exceed the above range. Through the quantitative comparison χ^2 values of different models, a better fitting model can be determined.

4. RESULTS AND DISCUSSION

By comparing the fitting results of the two different models, we found that the QENS spectra fitted with the rJRM model first has a wider range of neutron energy transfer and a higher range of scattering vectors($Q=0.3-1.9\,\text{Å}^{-1}$, $E=\pm 120\mu ev$). Secondly, the related physical parameters that describe the dynamic information of restricted water obtained by fitting are also more comprehensive. By the JRM model Eq.(1)-Eq. (5), the QENS spectra of M-S-H and C-S-H samples were fitted under temperature and scattering vector, five parameters of related physical quantities can be extracted, which are: the fraction of immobile (or bound) water, C, the translational diffusion coefficient, D_t , the rotational diffusion coefficient, D_r , the translational residence time, τ_0, and the Debye-Waller factor, A. These physical parameters can be divided into two categories, one reflects the structure of cement samples, such C, this is of great significance to the study of cement properties [31]; The other type reflects the dynamic information of restricted water, such as D_t , D_r , τ_0 , A , and the mean square displacement (MSD) calculated from the fitting parameter A. Similarly, By the rJRM model Eq.(1)-(2), Eq.(4) and Eq.(6)-(7), seven parameters related to the dynamics and confinement of water in these pastes can be extracted, in addition to the five parameters that are the same as the JRM model, the pore radius a_0 describing the micro-nanopores in the sample and the dimension deleted parameter x are added.

Figure 1. (a)-(d) shows the QENS spectra fitted by the rJRM and JRM models for the M-S-H samples when the temperature is 230K and 280K, and the Q values are both 0.5Å^{-1}. Figure 1. (a) and (b) are the fitting results of rJRM, and Figure 1. (c) and (d) are the fitting results of JRM. where red circle is the QENS spectra experimental data of the sample, blue solid line is the fitting curve, green dotted line ENS is the elastic scattering part of the QENS spectra, and black dashed line QENS is the inelastic scattering part (the QENS spectra broadening part). Similarly, Figure 2. (a)-(d) presents the QENS spectra results of rJRM and JRM model fitting when the temperature of C-S-H samples is 280K and Q value is 0.5Å^{-1} and 1.3Å^{-1} , respectively.

ISSN: 2472-3703 DOI: 10.6911/WSRJ.202105_7(5).0022

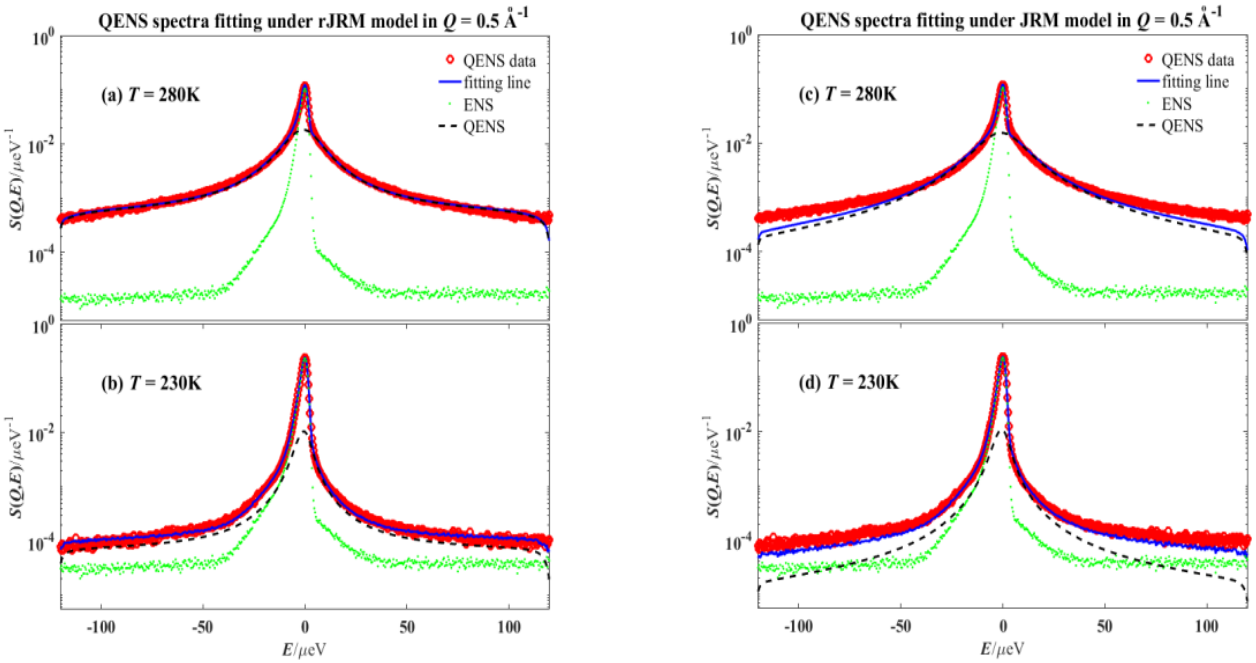

Figure 1. M-S-H QENS spectra data fitted by JRM and rJRM for temperatures 230K and 280K at Q values 0.5Å^{-1}, respectively. (a)(c) for 280K and (b)(d) for 230K.

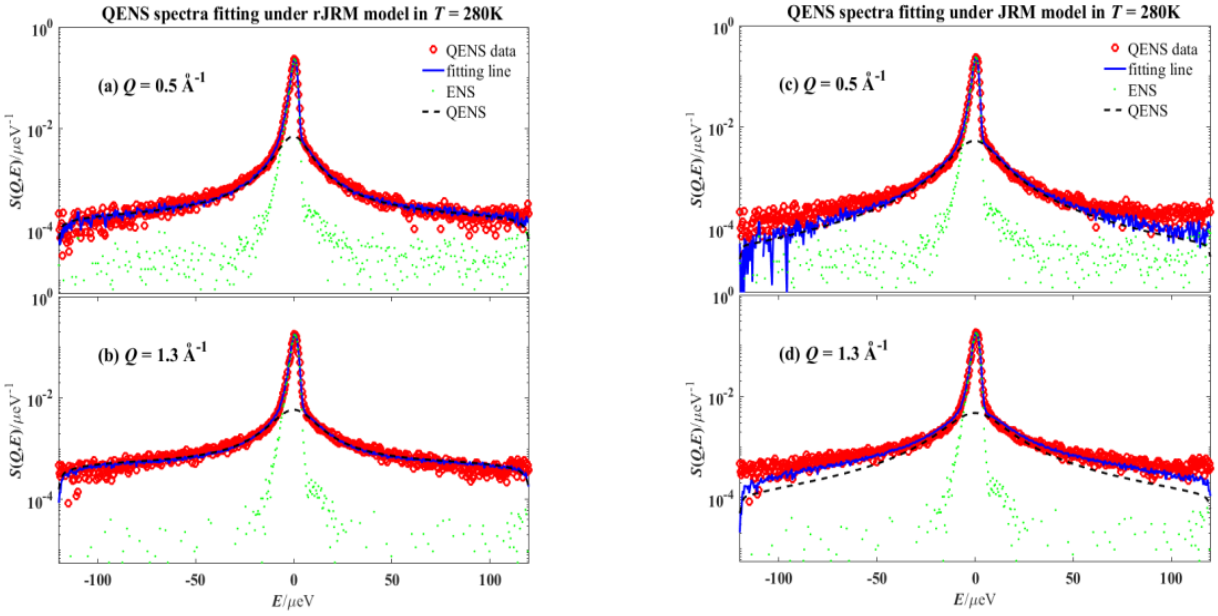

Figure 2. C-S-H QENS spectra data fitted by JRM and rJRM for Q values 0.5 Å^{-1} and 1.3Å^{-1} at temperatures 280K, respectively. (a)(c) Q = 0.5 Å^{-1} and (b)(d) Q = 1.3 Å^{-1}.

It can be seen from Figure 1 and Figure 2 that whether it is high temperature or low temperature, high Q or low Q, the blue fitting curve almost passes through the red experimental data points, but in Figure 1. (c) and Figure 2. (c), the fitting curve deviates significantly from the experimental data points at both ends of the QENS spectra (wider neutron energy transfer range), indicating that the JRM model has an unsatisfactory fitting effect for the QENS spectra of high temperature and low Q at higher neutron transfer energies, but in this case, the fitting effect of rJRM model in Figure 1.(a) and Figure 2.(a) is better. It can also be seen

ISSN: 2472-3703 DOI: 10.6911/WSRJ.202105_7(5).0022

from Figure 1 and Figure 2 that the ENS and QENS curves of the rJRM model are slightly higher than those of the JRM model. This is because ENS is the elastic scattering part of the neutron scattering spectra, and QENS is the inelastic scattering part. By substituting Eq.(3) and Eq.(5) into Eq.(1), there is only one term of ENS in JRM model, which comes from the chemically bound water combined in the hydrogen compound, and the QENS has two items, which come from the convolution when l takes different values in the translational diffusion function $S_T(Q,E)$ and the rotational diffusion function $S_R(Q,E)$; by substituting Eq.(6) and Eq.(7) into Eq.(1), the ENS of rJRM model has two terms, in addition to chemically bound water, there is also an elastic scattering part of movable water, and its QENS also adds a contribution of movable water to the inelastic scattering part.

Observe Figure 1. (a)(c) and (b)(d), the QENS spectral broadening at 280K is larger than that at 230K, and the $S(Q,E)$ value at both ends of E is larger. This is because the higher the temperature is, the more violent the movement of water molecules, the more water molecules in the pores tend to move, and the proportion of elastic scattering decreases, while the proportion of inelastic scattering increases. The elastic scattering spectra is the main part of the QENS spectra, which is concentrated in the range of wave peak, while the broadened part of the spectra is the inelastic scattering spectra. When the elastic scattering proportion decreases, the inelastic scattering proportion increases, the broadened QENS spectra becomes larger, and the $S(Q,E)$ values corresponding to both ends of the spectra are also larger. By comparing Figure 1.(a)(c) and Figure 2.(a)(c), it can be seen that at the same temperature and the same Q, the QENS spectra of M-S-H sample is wider and $S(Q,E)$ is also larger than that of C-S-H sample. In the same E, the QENS spectra data points of M-S-H sample are more clustered than that of C-S-H sample. This is because the structure of M-S-H sample is different from that of C-S-H sample. This is because the structure of M-S-H sample is different from that of C-S-H sample. The basic constituent unit of M-S-H sample is small particles and contains more nano-pores, so the proportion of confined water contained in the pores is larger and the inelastic scattering part reflected in QENS spectra is also larger.

During the QENS experiment in this paper, the number of measured values n is 600. Substituting the experimental data of QENS spectra $S_i(Q,E)$, the fitting value of QENS spectra $S_i^{'}(Q,E)$, and the error of the measured value σ_i into Eq.(8), the chi-square value can be obtained. Figure 3 shows the comparison of chi-square values of the QENS spectra fitted by rJRM and JRM model, the chi-square values vary with the neutron scattering vector. Where Figure 3. (a)(c) are the chi-square values of M-S-H samples, and Figure 3.(b)(d) are the chi-square values of C-S-H samples. Table3 lists the chi-square values of the QENS spectra fitted by rJRM and JRM models for M-S-H samples and C-S-H samples, and the temperatures at 280K and 230K, the Q values 1.1 $Å^{-1}$.

Table 3. Chi-square at Q =1.1 $Å^{-1}$

	Pure M-S-H		Pure C-S-H	
	280K	230K	280K	230K
rJRM	5.322x103	3.196x103	1.232x103	579.4
JRM	1.720x104	3.423x103	2.302x103	617.5

ISSN: 2472-3703 DOI: 10.6911/WSRJ.202105_7(5).0022

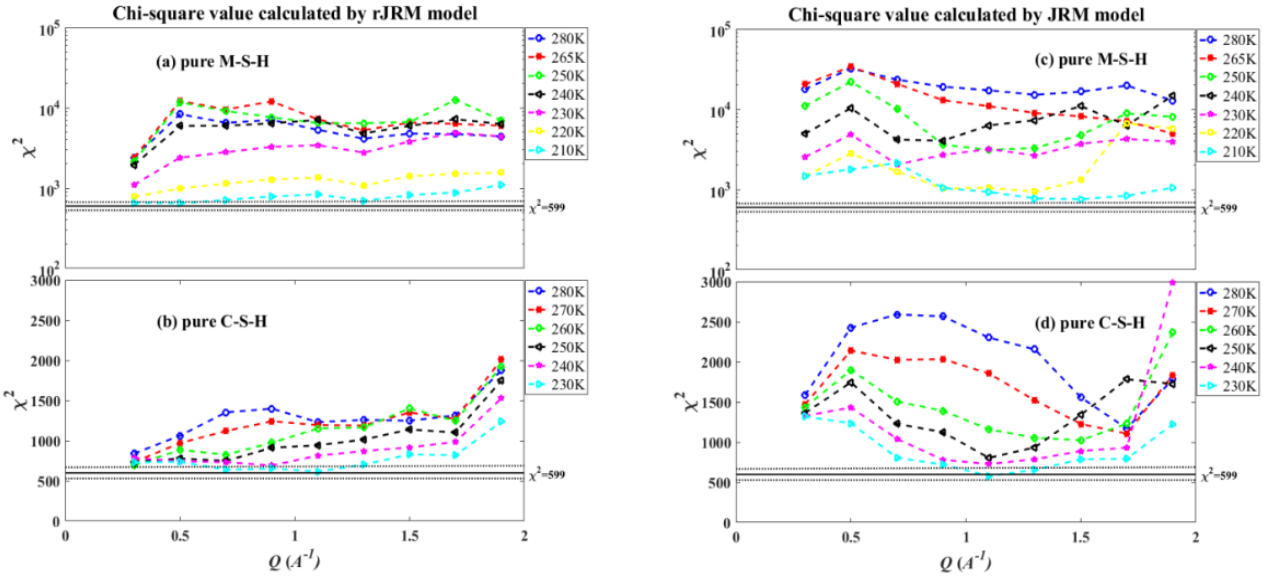

Figure 3. Chi-square values of QENS spectra fitted by rJRM and JRM models. (a)(c) for M-S-H and (b)(d) for C-S-H.

It can be seen from Figure 3 that the chi-square value obtained by the rJRM model as shown in Figure 3. (a)(b) is smaller than that obtained by the JRM model as shown in Figure 3. (c)(d). It can also be seen from Table 3 that when $Q = 1.1\,\text{Å}^{-1}$, the chi-square value of QENS spectra fitted by rJRM model at 280K and 230K is smaller than that of the JRM model. It indicates that whether it is M-S-H sample or C-S-H sample the deviation degree between the fitting value (theoretical value) of the rJRM model and the experimental data (measured value) of QENS spectra is smaller, and the fitting effect is better. which is also reflected in the rJRM curve of QENS spectra as shown in Figure 1 and Figure 2. It can also be seen from Figure 3. that the chi-square value of M-S-H sample given in Figure 3.(a)(c) is larger than that of C-S-H sample given in Figure 3.(b)(d). This is because the neutron scattering of the M-S-H sample reflects stronger signals in the QENS spectra than the C-S-H sample, and its measurement error is smaller, the test of the model is more accurate, and the subtle differences in the model can also be reflected in the chi-square value, so the chi-square value is larger.

The number of measured values n in this paper is 600. If the model has no deviation (ideal situation), the chi-square value is distributed in the range 599 ± 69.2 with a probability of 95%.

The three straight lines in Figure 3. (a)(b)(c)(d) represent the expected value and distribution range of Chi-square under ideal conditions. It can be seen from the figure that more chi-square values of the rJRM model fall within the range of the chi-square distribution under ideal conditions than that of the JRM model at low temperature, but the chi-square values of both the rJRM model and JRM model are higher than this range at high temperature. Chi-square values calculated by rJRM model or JRM model both fall within the range of Chi-square distribution under ideal conditions at low temperature, and the Chi-square values calculated by these two models falling within this range are different, which indicates that it is feasible to analyze and compare the advantages of the models by Chi-square. As the temperature increases, the chi-square value increases, indicating that there is still room for improvement in the fitted model, which is the direction of future model development. In general, the chi-square value of RJRM model is smaller than that of JRM model as a whole, and there are more chi-square data points in the range of chi-square distribution under ideal circumstances, indicating that rJRM model is more superior.

ISSN: 2472-3703 DOI: 10.6911/WSRJ.202105_7(5).0022

Table 4 lists the running time of fitting sample QENS data with different models in MATLAB. The calculation time is from the start of program operation to obtaining the corresponding physical parameters and fitting data $S'(Q,E)$, and the same computer is used to run under the same conditions.

From the table, we can see that for the same sample, the calculation speed by the rJRM model is much faster than the JRM model. This is because when aligning the Quasi-elastic neutron scattering spectra for nonlinear least-squares fitting, the superior model can reduce the number of iterations in the running process and find the optimal solution more quickly. Therefore, from the perspective of calculation time, it can also be seen that the rJRM model is more efficient in data processing.

Table 4. The calculation time of different models

	rJRM model	JRM model
Pure M-S-H	2.301s	15.81s
Pure C-S-H	2.396s	21.15s

5. CONCLUSIONS

To improve the performance of cement, the Quasi-elastic neutron scattering technique is used to analyze the water dynamics in cement. Different theoretical models are used to process the data of QENS experiment, and the results are quite different. To provide ideas for the improvement of subsequent models, this paper comprehensively analyzes the jump-diffusion and rotation-diffusion model (JRM) and the revised Jump-diffusion and rotating-diffusion model (rJRM). From the perspectives of model structure, model fitting results, model calculation time, and mathematical statistics law reveal the superiority of rJRM. The results show that: (1) the rJRM considers the structure of the model more comprehensively. The contribution of moving water to the elastic part is taken into account in the translational diffusion function part, and the contribution of neutron scattering length to the Sears expansion is taken into account in the rotational diffusion function part. (2) Fitting M-S-H samples and C-S-H samples at different Q and T conditions by rJRM model and JRM model, respectively. The fitting result image shows that the rJRM model not only has a wider fitting range and its fitting effect is much better than that of the JRM model but also can obtain more physical parameters describing the restricted water dynamics. (3) The chi-square value calculated by the rJRM model is also smaller than that of the JRM model, indicating that the deviation between the fitted data points and the experimental data points is smaller, and the quantitative description shows that the fitting effect is better. (4) The calculation time of each model can be obtained from MATLAB, and the calculation time of rJRM model is shorter, indicating that the model is more efficient in data processing.

ACKNOWLEDGMENTS

The research at MIT was supported by DOE grant no. DE-FG02-90ER45429 and partially by MIT/MISTI grant no. 2206012. E. F. and P. B. acknowledge partial financial support from Consorzio Interuniversitario per lo Sviluppo dei Sistemi a Grande Interfase (CSGI) and “Progetto Dipartimenti di Eccellenza 2018-2022” allocated to Department of Chemistry “Ugo Schiff” from MIUR, for financial support. Authors kindly thank Dr. P. Le for providing M-S-H and C-S-H QENS data.

ISSN: 2472-3703 DOI: 10.6911/WSRJ.202105_7(5).0022

REFERENCES

[1] Mindess S, Young J F, Darwin D. Concrete[J]. Prentice Hall, 2003.

[2] Gartner E M, Macphee D E. A physico-chemical basis for novel cementitious binders[J]. Cement and Concrete Research, 2011, 41(7): 736-749.

[3] Chiang W S, Ferraro G, Fratini E, et al. Multiscale structure of calcium- and magnesium-silicate-hydrate gels[J]. Journal of Materials Chemistry A, 2014, 2(32): 12991-12998.

[4] Vandeperre L J, Liska M, Al-Tabbaa A. Hydration and Mechanical Properties of Magnesia, Pulverized Fuel Ash, and Portland Cement Blends[J]. Journal of Materials in Civil Engineering, 2008, 20(5): 375-383.

[5] Ridi F, Fratini E, Baglioni P. Cement: A two thousand year old nano-colloid[J]. Journal of Colloid And Interface Science, 2011, 357(2).

[6] Allen A J, Thomas J J, Jennings H M. Composition and density of nanoscale calcium-silicate-hydrate in cement[J]. Nature Materials, 2007, 6(4): 311-6.

[7] Bordallo H N, Aldridge L P, Desmedt A. Water Dynamics in Hardened Ordinary Portland Cement Paste or Concrete:? From Quasielastic Neutron Scattering[J]. Journal of Physical Chemistry B, 2006, 110(36): 17966-17976.

[8] Ridi F, Luciani P, Fratini E, et al. Water Confined in Cement Pastes as a Probe of Cement Microstructure Evolution[J]. Journal of Physical Chemistry B, 2009, 113(10): 3080-7.

[9] Skinner L B, Chae S R, Benmore C J, et al. Nanostructure of Calcium Silicate Hydrates in Cements[J]. Physical Review Letters, 2010, 104(19): 195502.

[10] Eckold G, Nagler S E. Studying Kinetics with Neutrons[M]. Springer, 2010.

[11] Chen S H, Liao C, Sciortino F, et al. Model for single-particle dynamics in supercooled water[J]. Physical Review E, 1999, 59(6): 6708-6714.

[12] Fratini E, Chen S H, Baglioni P, et al. Quasi-elastic neutron scattering study of translational dynamics of hydration water in tricalcium silicate[J]. The Journal of Physical Chemistry B, 2002, 106(1): 158-166.

[13] Harris D H C, Windsor C G, Lawrence C D. Free and bound water in cement pastes[J]. Magazine of Concrete Research, 1974, 26(87): 65-72.

[14] Thomas J J, Fitzgerald S A, Neumann D A. The state of water in hydrating tricalcium silicate and Portland cement pastes as measured by quasi-elastic neutron scattering[J]. Journal of the American Ceramic Society, 2001, 84(8): 1811-1816.

[15] Le P, Fratini E, Zhang L, et al. Quasi-elastic neutron scattering study of hydration water in synthetic cement: An improved analysis method based on a new global model[J]. The Journal of Physical Chemistry C, 2017, 121(23): 12826-12833.

[16] Hua Li, Yu-Hang Chen, Bin-Ze Tang. A revised jump-diffusion and rotation-diffusion model[J]. Chinese Physics B, 2019(5): 216-221.

[17] Peisi L, Fratin E, Zhang L, et al. Quasi-Elastic Neutron Scattering Study of Hydration Water in Synthetic Cement: An Improved Analysis Method Based on a New Global Model[J]. The Journal of Physical Chemistry C, 2017.

[18] Bellissent-Funel M-C, Chen S, Zanotti J-M. Single-particle dynamics of water molecules in confined space[J]. Physical Review E, 1995, 51(5): 4558.

[19] Mamontov E, Herwig K W. A time-of-flight backscattering spectrometer at the Spallation Neutron Source, BASIS[J]. Review of Scientific Instruments, 2011, 82(8): 61.

ISSN: 2472-3703 DOI: 10.6911/WSRJ.202105_7(5).0022

[20] Zhang Y, Lagi M, Liu D, et al. Observation of high-temperature dynamic crossover in protein hydration water and its relation to reversible denaturation of lysozyme[J]. Journal of Chemical Physics, 2009, 130(13): 04B601-332.

[21] Li H, Fratini E, Chiang W S, et al. Dynamic behavior of hydration water in calcium-silicate-hydrate gel: A quasielastic neutron scattering spectroscopy investigation[J]. Physical Review E, 2012, 86(6-1): 061505.

[22] Le P, Fratini E, Ito K, et al. Dynamical behaviors of structural, constrained and free water in calcium- and magnesium-silicate-hydrate gels[J]. Journal of Colloid & Interface Science, 2016, 469: 157-163.

[23] Teixeira J, Bellissent-Funel M C, Chen S H, et al. Experimental Determination of the Nature of Diffusive Motions of Water Molecules at Low Temperatures[J]. Physical Review A, 1985, 31(3): 1913-1917.

[24] Sears V. Theory of cold neutron scattering by homonuclear diatomic liquids: II. Hindered rotation[J]. Canadian Journal of Physics, 1966, 44(6): 1299-1311.

[25] Singwi K, Sjölander A. Diffusive motions in water and cold neutron scattering[J]. Physical Review, 1960, 119(3): 863.

[26] Li H, Zhang L-L, Yi Z, et al. Translational and rotational dynamics of water contained in aged Portland cement pastes studied by quasi-elastic neutron scattering[J]. Journal of colloid and interface science, 2015, 452: 2-7.

[27] Wang Z, Le P, Ito K, et al. Dynamic crossover in deeply cooled water confined in MCM-41 at 4 kbar and its relation to the liquid-liquid transition hypothesis[J]. The Journal of chemical physics, 2015, 143(11): 114508.

[28] Viani A, Zbiri M, Bordallo H N, et al. Investigation of the setting reaction in magnesium phosphate ceramics with quasielastic neutron scattering[J]. The Journal of Physical Chemistry C, 2017, 121(21): 11355-11367.

[29] Lancaster H O, Seneta E. Chi-square distribution[J]. Encyclopedia of biostatistics, 2005, 2.

[30] Satterthwaite F E. Synthesis of variance[J]. Psychometrika, 1941, 6(5): 309-316.

[31] Neville A M. Properties of concrete[M]. 4. Longman London, 1995.